ELSEVIER

Ceramics International 26 (2000) 745–751

CERAMICS INTERNATIONAL

# The use of impedance spectroscopy in damage detection in tetragonal zirconia polycrystals (TZP)

Andy Tiefenbach [a,*], Susanne Wagner [b], Rainer Oberacker [b], Bernd Hoffmann [a]

[a] *Institut für Werkstoffe der Elektrotechnik (IWE), Universität Karlsruhe (TH), Adenauerring 20, 76131 Karlsruhe, Germany*
[b] *Institut für Keramik im Maschinenbau (IKM), Universität Karlsruhe (TH), Haid und Neustraße 7, 76131 Karlsruhe, Germany*

Received 28 July 1999; received in revised form 21 September 1999; accepted 2 November 1999

**Abstract**

Tetragonal zirconia polycrystals (TZP) were chosen as a model material for evaluating the potential of impedance spectroscopy (IS) as a non-destructive method for the detection of microstructural damage. Cracks were introduced and propagated in these materials either by thermally induced phase transformation or by mechanical loading of pre-cracked specimens. In TZP, microcracking, its propagation and concomitant phase transformations were detected as changes in the capacitive and resistive parts of the electrical impedance at temperatures between 20 and 550°C. This can be correlated with in situ observation by optical microscopy of crack opening and phase transformation zones in four point bending test specimens. Qualitatively all aspects of microcracking described above have been shown to be measurable by IS. Quantitative sensitivity limits in terms of error bands and critical crack lengths are derived from the experimental results and numerical field simulations. 

*Keywords:* C. Impedance; Damage detection

## 1. Introduction

The use of ceramic materials as structural components is often hindered by reliability problems resulting from static or cyclic fatigue. Therefore, methods have to be developed for non destructive detection of defects before these defects reach a critical size. Electrical measurements offer some advantages over to the more common NDE methods, such as in situ monitoring and local measurement of the critical component sections. There is, however, only limited information available on the application of methods such as impedance spectroscopy for this purpose [1]. No assessment of the potential of electrical methods is possible on the basis of the present knowledge.

Ionic conductors such as zirconia seem to be suitable materials for this technique. Zirconia is used in structural applications mainly in the form of partially stabilized zirconia (PSZ), or tetragonal zirconia polycrystals (TZP) [2]. PSZ thermal barrier coatings and PSZ or TZP cutting devices are typical applications, where long term failure can occur by fatigue. In these applications, damage detection prior to catastrophic failure could prevent dramatic consequences.

The aim of the present work was to study the influence of cracks and the influence of the tetragonal (t) to monoclinic (m) phase transformation, which accompanies crack propagation in PSZ and TZP, on the electrical impedance of the specimens, in order to evaluate the potential of impedance spectroscopy as a new NDE method for damage detection. Ce-stabilized TZP was chosen as a model material. This material develops large transformation zones at crack tips, which can be expected to give an additional contribution to impedance changes during crack propagation.

## 2. Experimental procedure

### 2.1. Sample preparation

$ZrO_2$-powder containing 9 mol% $CeO_2$ (9Ce-TZP, Unitec, UK) was used as starting material. The powder was compacted into plates of 65×45×12 mm by axial pre-compacting and subsequent cold isostatic pressing

* Corresponding author. Fax: +49-721-608-7492.

0272-8842/00/$ - see front matter 
PII: S0272-8842(00)00014-6

at 400 MPa. Sintering was carried out at 1400°C for 2 h in air. The required specimen shapes were manufactured from the plates by diamond cutting and grinding. All specimens were annealed at 1200°C for 1 h to remove the monoclinic zone at the surface, induced by grinding.

### 2.2. Characterisation of microstructure and phase transformation

SEM and TEM were utilized for investigating the microstructure. The mean grain size was determined from SEM micrographs by linear analysis. Samples for TEM investigations were prepared by grinding, dimpling and ion milling. A Zeiss EM912 Omega microscope with an accelerating voltage of 120 kV was used for TEM investigations. Phase analysis was carried out by XRD, using Cu-$K_\alpha$ radiation. The monoclinic fraction was derived from the $(11\text{-}1)_m$, $(111)_m$ and $(111)_t$ - peaks according to Toraya [3].

The t→m transformation was studied by applying strain gauges to the specimens and cooling them down to −85°C in silicon oil inside a bath kryostat. The reverse m→t transformation was studied by heating of the transformed specimens in a Netzsch 402-dilatometer. The heating and cooling rate was set to 2 K/min in these experiments.

### 2.3. Electrical measurements

The required electrodes were prepared by vacuum deposition of chromium/nickel for room temperature measurements and of platinum for all other experiments. At room temperature the sample capacitance was measured by a multi-frequency LCR Meter (HP 4275A, Hewlett Packard) over a frequency range from 10 kHz to 10 MHz. In the temperature range from 150 to 550°C an impedance analyser (SI 1260, Solartron) was used over a frequency range from 1 Hz to 1 MHz. The samples were heated by high-intensity infrared line heaters. All experiments were performed in air. The specimen size for experiments with unloaded samples was 10×8×12 mm.

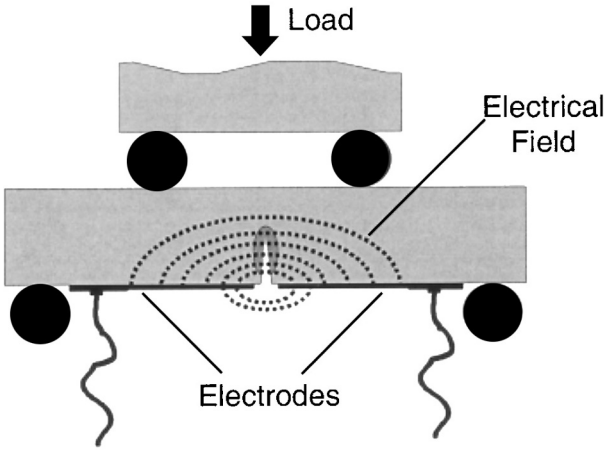


Fig. 1. In situ impedance spectroscopy characterisation.

Room temperature IS measurements were also carried out in situ on mechanically loaded samples. The classical four point bending experiment with an inner and outer span of 20 and 40 mm, respectively (Fig. 1) was chosen to study the influence of crack opening on the electrical behaviour of the specimens. Bending bars of 9×4×45 mm with a sharp starting crack were exposed to loading- unloading cycles with increasing load level. The crack length was monitored by an optical microscope. The permittivity of the specimens was measured during the constant load and the corresponding deloading part of each cycle using the electrode arrangement given in Fig. 1. This arrangement was designed for maximum sensitivity, although it does produce an inhomogeneous electrical field and thus numerical modelling is required for quantitative analysis. This modelling was performed using the software code MAFIA [4].

## 3. Results

### 3.1. Microstructure of the starting material

The mean grain size of the investigated zirconia material was calculated to be 1.1 μm. The TEM micrograph (Fig. 2a) shows tetragonal grains, monoclinic twins in a tetragonal grain and an intergranular phase of approximately 80 nm in size situated at the triple points. Fig. 2b shows a higher resolution of a grain boundary in 9Ce-TZP. The figure indicates the existence of a continuous thin grain boundary phase with a maximum thickness of 1.7 nm.

The XRD measurements revealed a single phase tetragonal microstructure, indicating that the monoclinic twins in the TEM specimens are caused by the grinding operation during specimen preparation. This single phase tetragonal microstructure in the as annealed state will be referred to as the reference state of the material.

### 3.2. Thermally induced transformation behaviour of 9Ce-TZP

The length change during cooling to −85°C and subsequent heating up to 500°C is shown in Fig. 3.

The t→m transformation occurs spontaneously at the so called "Martensitic burst"- temperature $M_b$. From XRD measurements it was determined that 80% of the t-phase is transformed to the monoclinic at $M_b$. No significant increase in the monoclinic fraction was observed during further cooling from $M_b$ to −85°C. The

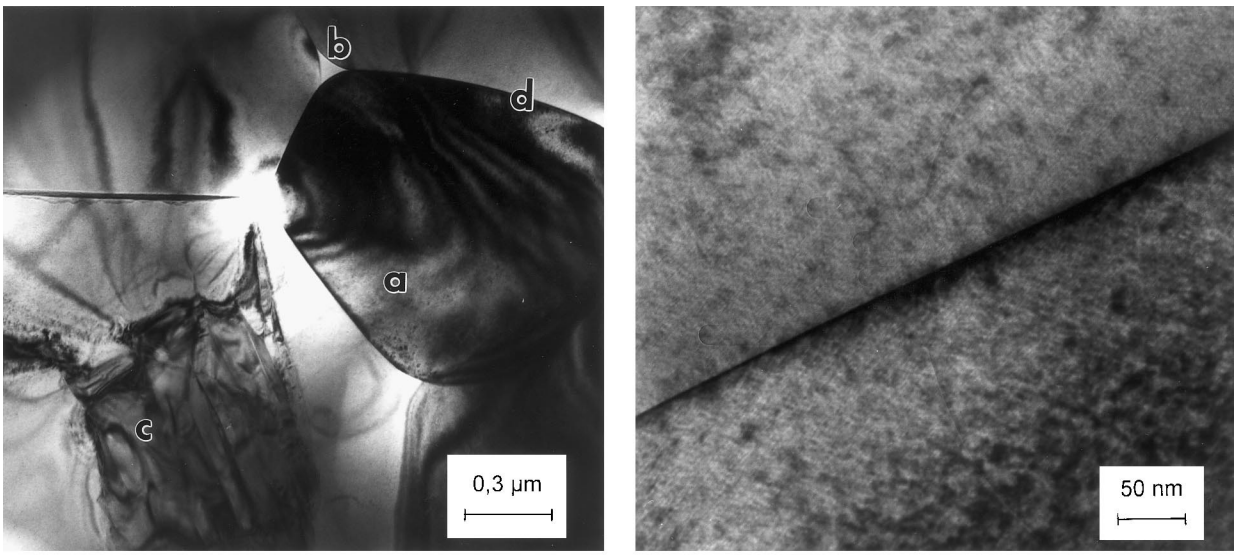


(a) (b)

Fig. 2. (a). TEM micrograph of tetragonal zirconia with (a) tetragonal grains, (b) grain boundary phase in triple point, (c) monoclinic twins in tetragonal grain, (d) grain boundary; (b) grain boundary phase in 9Ce-TZP.

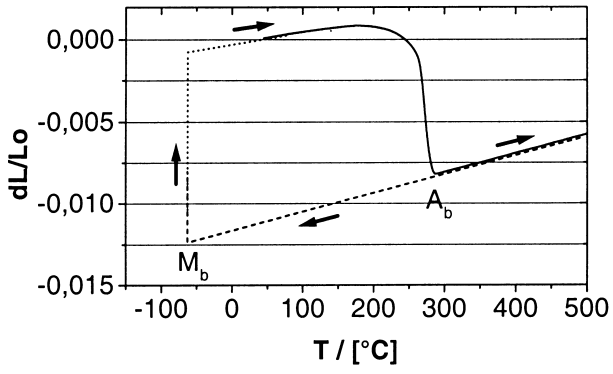


Fig. 3. Relative length change $\Delta L/L_0$ during cooling of tetragonal 9Ce-TZP to the martensitic burst temperature $M_b$ and subsequent heating.

reverse transformation m→t takes place over an extended temperature interval and causes a linear contraction of about 1%. However, the main part of the transformation reaction is observed close to the "Austenite"- temperature $A_b$, at which the transformation is complete. Both $M_b$ and $A_b$ increase with the grain size of the material, a detailed study of which will be published elsewhere [5]. For the materials used in the present work, −60 and +290°C were observed for $M_b$ and $A_b$, respectively.

The expansion during t→m transformation causes severe crack formation in the specimens. The cracks are not healed during subsequent heating beyond $A_b$. Thus, two additional types of microstructure could be produced besides the undamaged tetragonal reference state: (a) a 80% monoclinic/20% tetragonal microstructure with a high crack density produced by cooling below $M_b$; (b) a fully tetragonal microstructure with the same crack density, produced by heating of the thermally transformed specimens to temperatures beyond $A_b$.

### 3.3. Permittivity of 9Ce-TZP in the tetragonal reference state and after thermally induced phase transformations

Preliminary electrical measurements for the 9Ce-TZP material were carried out at room temperature. Impedance spectra were recorded: first on the undamaged tetragonal reference state; second, after the t→m transformation with concomitant cracking induced by cooling; and third, after reversing the transformation by heating beyond $A_b$. The resulting changes in the electrical properties were observed as differences in the capacitive part of the impedance. Table 1 compares the effective permittivities at a frequency of 1 MHz evaluated from the measured sample capacitances.

After t→m transformation a reproducible, drastic decrease of the effective permittivity can be detected, and amounts to −30%. After m→t re-transformation one observes almost the same permittivitiy as in the reference state. This indicates that the phase transformation t→m is predominantly responsible for the decrease in the permittivity, despite the fact that severe damage in form of macro- and microcracks is present in the entire sample volume. However, the volume fraction of the cracks is negligible. Hence, cracks have only an insignificant influence on the permittivity at room temperature as long as they are closed. The considerable decrease in permittivity due to the phase transformation is caused presumably by the change of crystal structure or by the appearance of textures.

Table 1
Permittivity of 9Ce-TZP before and after thermally induced phase transformations

| 9Ce-TZP (microstructure) | Effective permittivity $\varepsilon$ |
|---|---|
| Crack free tetragonal (100%t) reference state | 38.1 |
| After cooling $< M_b$ (cracks, 80%m/20%t) | 26.7 |
| After reheating $> A_b$ (cracks, 100%t) | 38.0 |

### 3.4. Electrical properties of 9Ce-TZP in the temperature range from 150 to 550°C

In the temperature range up to 550°C, TZP is a pure ionic conductor [6]. In order to gain more information about the effects of microstructure on electric properties, impedance spectra were recorded at elevated temperatures for the three types of microstructure mentioned above.

The analysis of the Bode characteristics shown in Fig. 4a indicates the presence of two polarizations in the tetragonal reference state. Impedance spectra recorded on specimens with variable length $L$ and four terminal d.c. conductance measurements proved that electrode polarization does not appear in the spectrum in the frequency range 1 Hz to 1 MHz. Therefore the existence of the two well separated mechanisms above 250°C corresponds to a two-phase electrolyte behaviour.

Comparing the tetragonal reference samples with the samples after t→m→t transformations, the closed cracks in the transformed and subsequently re-transformed samples turn out to influence the electrical properties significantly. Fig. 4b shows the impedance spectra for 9Ce-TZP of both microstructures. Changes occur only in the low-frequency range, where the conductivity of the crack containing material is clearly reduced compared to that of the reference state.

In order to find qualitative and quantitative correlations between the microstructures and the electrical properties, it is useful to fit the Bode characteristics to an appropriate equivalent circuit and to estimate the values of the circuit parameters. An idealized but often effective model, which has been termed brick layer model [7], treats the microstructure as an array of cubic-shaped grains, separated by plane grain boundaries. An alternative is the model proposed by Schouler [8] for materials with intergranular contact. We use the brick layer model because of the existence of a continuous grain boundary phase in our materials. The circuit parameters are obtained by least square fitting.

The normalized capacitances, $c=(L/A)\cdot C$, which are numerically independent of the specimen geometry, were all found to be independent of temperature (Fig. 5a). Comparing the two capacitances in the reference state, the smaller capacitance $c_{gi}$, which equals almost the sample capacitance at room temperature corresponds to the volume fraction of the grains. From the ratio of both values, one can estimate the layer thickness of the grain boundary phase to 2.5 nm, if $\varepsilon_{gi} = \varepsilon_{gb} = 38$ and an average grain size of 1.1 μm are assumed. This is in good agreement with the results of the TEM investigations. The crack damage due to t→m→t transformations does not alter the grain interior capacitance $c_{gi}$. On the other hand, the grain boundary capacitance $c_{gb}$ decreases clearly compared to the reference value. One possible explanation is that the cracks in this material reduce primarily the effective permittivity of the grain boundary volume.

The conductivity in the grains and in the grain boundary phase is thermally activated as seen in the Arrhenius plots (Fig. 5b). Compared with the grain boundary phase, the grain conductivity is much higher. Cracking has no significant influence on the activation energies for the grain interior. However, cracking clearly reduces the conductivity in the grain boundary phase. Additionally, there is a considerable change in the activation energy.

In the monoclinic state, zirconia can only be characterized at temperatures below $A_b$. In this experiment we examined samples after the t→m transformation; these contain 80% of the monoclinic phase. In terms of

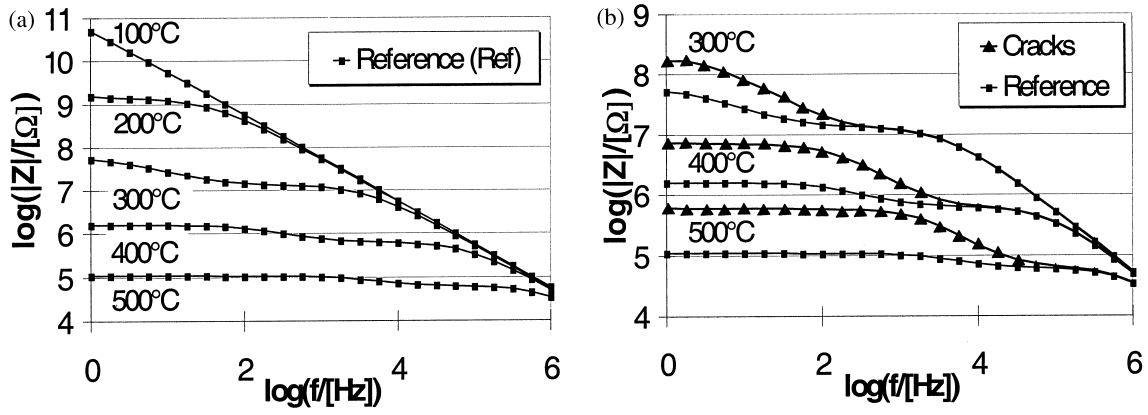


Fig. 4. Impedance spectra for 9Ce-TZP in the reference state and after t→m→t transformations.

the brick layer model, only the capacitive-resistive electrolyte polarization corresponding to the grain interior can be observed in this temperature range. As shown in Fig. 6a the grain capacitance of the material is constant up to 240°C and then increases up to the value of the single phase tetragonal microstructure. This is obviously due to the m→t phase transformation taking place in the temperature interval from 240 to 290°C, which is consistent with the results from dilatometer measurements. Fig. 6b compares the conductivity of the two different crystal structures. The conductance of monoclinic grains is reduced compared to the tetragonal reference state. Thus, the electrical properties of the two structures differ in permittivity as well as in conductivity.

### 3.5. *In situ permittivity measurements on bending specimens under mechanical load*

Under mechanical load, crack opening occurs, increasing the crack volume and thus contributing to a reduction in permittivity. In situ experiments were carried out in order to study this effect quantitatively. Fig. 7 shows the result of one of these experiments, where a pre-cracked bending bar with a starting crack of length $a = 2.67$ mm was subjected to loading/unloading cycles with increasing peak load. The relative capacitance of the arrangement under load (Fig. 7a) decreases monotonously with increasing load. After relieving the load, the capacitance increases, but remains somewhat below the capacitance measured at the beginning of the experiment. The relief curve shows a residual loss in capacitance with increasing peak load. This loss in capacitance in the unloaded state increases after exposure to peak load levels, where crack growth takes place (Fig. 7b).

It is probably caused by a monoclinic transformation zone at the crack tip. The relative capacitance under load decreases more than 5% as the crack length increases from 2.67 to 3.5 mm. Qualitatively, this decrease in capacitance correlates with the experimentally observed crack length $a$ (Fig. 7b) and the calculated crack opening $COD$. This aspect will be treated more in detail in the discussion part of this paper.

## 4. Discussion

The experiments show that the electrical properties of the investigated 9Ce-TZP are affected significantly by its phase composition and the presence of cracks in the microstructure. Thus, detection of mechanically induced damage by impedance spectroscopy is possible, in principle. At room temperature, where only the capacitive part of the impedance is measurable, changes of about 0.1% can be significantly detected. The t→m phase transfor-

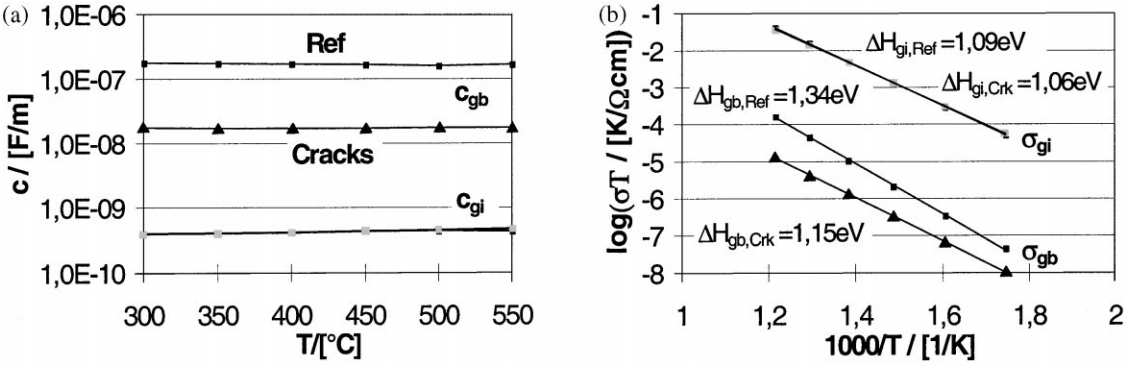


Fig. 5. Capacitance and conductivity (according to the brick layer model) for 9Ce-TZP in the reference state and after t→m→t transformations.

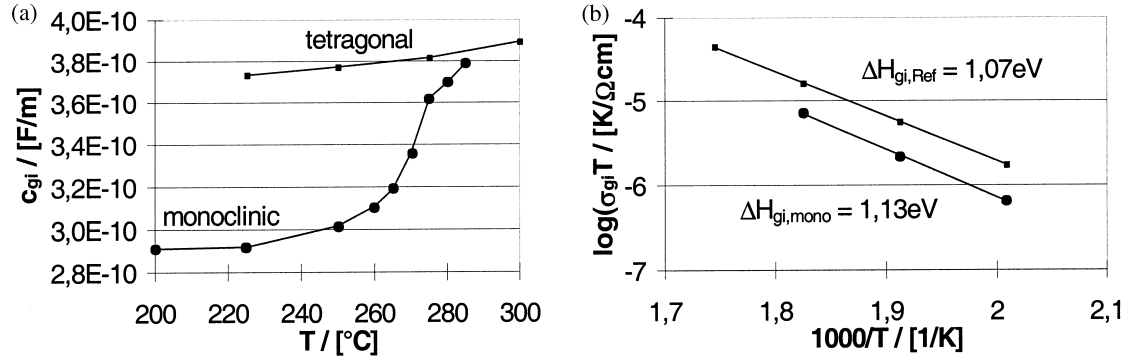


Fig. 6. Capacitance and conductivity of tetragonal and monoclinic grains.

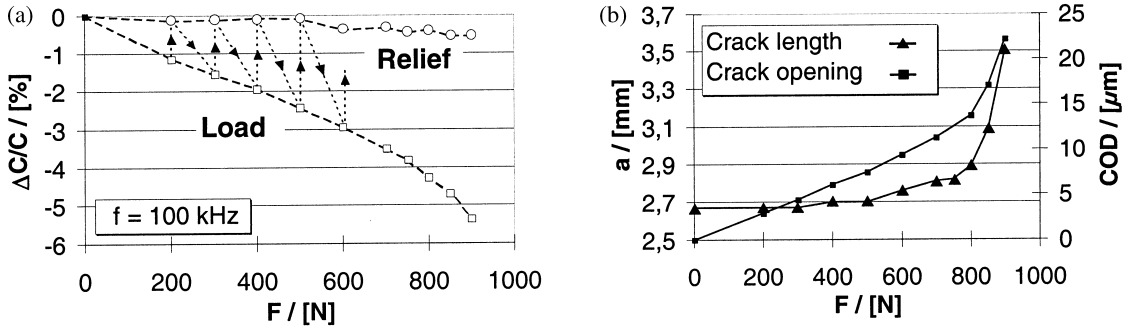


Fig. 7. In situ impedance spectroscopy for the study of crack opening and crack growth in four point bending.

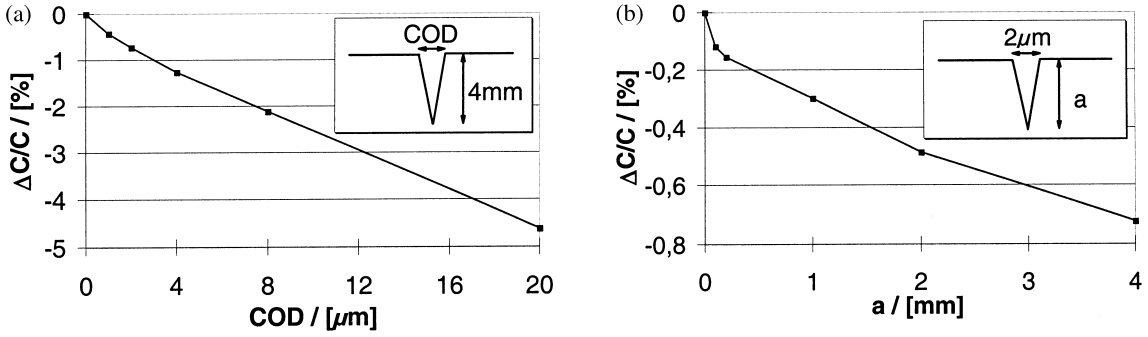


Fig. 8. Numerical simulation of the capacitance decrease depending on crack geometry.

mation results in a 30% drop in permittivity and thus becomes significant, if the monoclinic fraction is greater then 0.3% within a homogeneous sample. Closed cracks, however, do not result in detectable permittivity changes.

Under external load, cracks open resulting in a reduction in capacitance as demonstrated in the bending experiment. The electrical response of such cracks depends on the electrode arrangement with respect to the crack. It can be derived from numerical field simulations for the investigated configuration, which were carried out assuming the specimen to be an ideal, homogeneous dielectric with an effective permittivity of 38. As shown in Fig. 1, the crack is modelled as a trigonal wedge filled with air of a relative permittivity of 1. The electrodes are assumed to be ideal conductors. The distance between the electrodes is 3 mm, corresponding to the experimental conditions.

For a constant crack length of e.g. 4 mm, the relative capacitance decreases with increasing crack opening as shown in Fig. 8a. The calculated capacitive loss is in fair agreement with the experiment, indicating that crack configurations can be derived from the measured capacitance loss by numerical electric field modelling. Calculations based on the exact experimental crack configurations and monoclinic process zones at the crack tip are being carried out at present and will be published later.

Fig. 8b shows the relative change in capacitance for a small crack opening of 2 μm (low load) versus crack length. Given that the measuring accuracy is 0.1%, a crack length of 100 μm seems to be detectable. Thus, relatively short cracks under low load could be detected. The sensitivity of the method can further be increased by reducing the distance between the electrodes.

A much higher potential for crack detection in this type of structural ceramics arises from measurements at elevated temperatures. The impedance spectra measured in this work show a very significant reduction in the ionic conductivity, when cracks are present in the material, even if these cracks seem to be completely closed. Also the crystal structure and thus phase transformations, which accompany cracks in these materials can be easily detected. However, the interpretation of the measured impedance spectra with respect to microstructure requires further experiments and modelling activities.

## Acknowledgements

This work was funded by the German National Science Foundation (DFG) under contract No. Ho 693/11-12 and Ob 104/4-2. We would also like to thank Mr. Fotouhi for the support during TEM investigations.

## References


[1] M. Kleitz, C. Pescher, L. Dessemond, Impedance spectroscopy of microstructure defects and crack characterisation, Science and Technology of Zirconia 5 (1993) 593–608.

[2] D.J. Green, R.H.J. Hannink, M.V. Swain, Transformation Toughening of Ceramics, CRC Press, Boca Raton (FL), 1989.

[3] H. Toraya, M. Yoshimura, S. Somiya, Calibration curve for quantitative analysis of the monoclinic-tetragonal $ZrO_2$ system by X-ray diffraction, J. Am. Ceram. Soc. 67 (1984) 183–184.

[4] T. Weiland, MAFIA Software-Dokumentation, 1992.

[5] A. Tiefenbach, R. Oberacker, Measurement of m→t transformation in Ce-TZP by dilatometry and impedance spectroscopy, in preparation.

[6] A. Barhmi, E. Schouler, A. Hammou, M. Kleitz, Electrical Properties of Tetragonal Partially Stabilized Zirconia, Adv, In Ceramics 24B (1985) 885–894.

[7] A.J. van Dijk van Dijk van DijkBurggraaf, , Grain Boundary Effects on Ionic Conductivity in Ceramic $Gd_xZr_{1-x}O_{2-(x/2)}$ Solid Solutions, Phys. Stat. Sol. (a) 63 (1981) 229–240.

[8] E.J. Schouler, Etude des Cellules a Oxyde Electrolyte par la Methode des Impe-dances Complexes, Ph.D. thesis, Institut National Polytechnique de Grenoble, 1979.